JOURNAL OF OPTOELECTRONICS AND ADVANCED MATERIALS Vol. 9, No. 1, January 2007, p. 18 - 23

Invited Lecture

Theoretical investigation of the organic light-emitting diode activated by nanocrystal quantum dots

K. KOHARY[a*], V. M. BURLAKOV[a,b], D. G. PETTIFOR[a]
[a]*Department of Materials, University of Oxford, Parks Road, Oxford, OX1 3PH, United Kingdom*
[b]*Institute for Spectroscopy Russian Academy of Sciences, Troitsk, Moscow region, 142190, Russia*

We have developed a rate equation model to study the light emission intensity and quantum efficiency of an organic light-emitting diode (OLED), in which the emissive layer of nanocrystals (NCs) is embedded between the electron and hole transport layers of organic semiconductors, e.g. at the organic-organic interface. We have found that the NC-OLED light emission intensity and quantum efficiency are mainly affected by the efficiency of the Förster injection of excitons into the nanocrystals from the organic-organic interface, and they are less sensitive to the exciton diffusion at this interface. We have shown that there is an optimum concentration of nanocrystals, at which the light emission intensity reaches its maximum, while the quantum efficiency of the NC-OLED decreases monotonically with the nanocrystal concentration.

(Received November 28, 2006; accepted December 21, 2006)

Keywords: Organic light-emitting diode, Förster energy transfer, Nanocrystals

1. Introduction

A hybrid device of an organic light-emitting diode (OLED) incorporating nanocrystal (NC) quantum dots has recently been suggested as a new form for solid state lighting [1,2,3]. This hybrid NC-OLED capitalizes on the high radiative recombination efficiency of excitons and the low emission line broadening of inorganic nanocrystals, in addition to the low cost fabrication of semiconductor organic films as transport materials. In this paper, we analyse the favourable device architecture of the NC-OLED [4], when a monolayer of nanocrystals is embedded between the hole and electron transport layers of organic semiconductor films, e.g. at the organic-organic interface, as shown in Fig. 1.

A model of a NC-OLED should account for at least four different physical processes: the charge carrier transport through the organic semiconductors to the organic-organic interface, the exciton formation and exciton kinetics at the organic-organic interface, the exciton injection into the nanocrystals, and the light emission by nanocrystals (Fig. 1). In the past, all these processes have been studied separately [5,6,7]. In this paper, we develop a model which combines the above mentioned processes describing the basic characteristics of the NC-OLED. The objective is to study the NC-OLED light emission intensity and quantum efficiency as a function of the nanocrystal concentration at the organic-organic interface, in order to help the design of the NC-OLED. For simplicity, we assume that the nanocrystals form a regular hexagonal lattice at the two-dimensional organic-organic interface and that the spacing between the nanocrystals may be changed, for example, by using different sized bridging ligands. Recently, a nanocrystal array of CdSe quantum dots, which are cross-linked by different sized oligomers, has been fabricated and characterized [5].

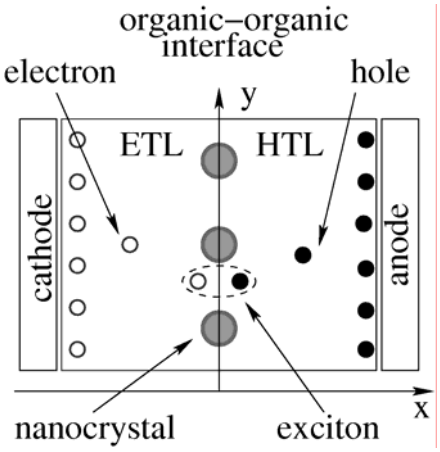

Fig. 1. Schematic picture of an organic light- emitting diode incorporating nano crystals at the organic-organic interface (NC-OLED).

2. Rate equation model

We employ a rate equation model to study the light emission by the nanocrystals in the NC-OLED:

$$\frac{dN_0}{dt} = -CN_0 + \frac{N_1}{\tau}, \tag{1}$$

$$\frac{dN_1}{dt} = CN_0 - \frac{N_1}{\tau}, \tag{2}$$

$$N_0 + N_1 = \rho, \tag{3}$$

where N_0 and N_1 are the concentrations of empty nanocrystals and nanocrystals containing one exciton, respectively, C is the exciton injection rate into the nanocrystals from the organic-organic interface, $1/\tau$ is the recombination rate of excitons in the nanocrystals, and ρ is the concentration of nanocrystals at the organic-organic interface. In the NC-OLED, the exciton injection rate into the nanocrystals, C, is determined by the efficiency of the Förster injection of excitons from the organic-organic interface into the nanocrystals. This latter process is affected by the exciton kinetics at the organic-organic interface, which is described in Sec. 2.1. The charge transport in organic semiconductors determining the exciton formation rate and therefore the exciton kinetics is investigated in Sec. 2.2. In our model of the NC-OLED, we assume that the nanocrystals are capped by a monolayer wide band gap inorganic material and/or by a layer of organic ligands that have a much larger energy gap than the nanocrystal. The latter capping layers have been demonstrated to inhibit charge injection [8], so that they act as injection barriers for electrons and holes into the nanocrystals. In addition, we assume that no excitons can be generated or formed in the capping layer of nanocrystals.

2.1. Exciton kinetics

The exciton injection rate into nanocrystals is determined by the exciton kinetics at the organic-organic interface. The exciton kinetics can be described analytically along the organic-organic interface for a low concentration of nanocrystals ($\rho \to 0$). We then discuss the numerical approach to determine the exciton injection rate at other nanocrystal concentrations at the organic-organic interface.

It is helpful to write the diffusion equation for the exciton concentration n_{exc} for an isolated nanocrystal. It is given by

$$\frac{\partial n_{exc}(r,t)}{\partial t} = \frac{D_{exc}}{r}\frac{\partial}{\partial r}\left(r\frac{\partial n_{exc}(r,t)}{\partial r}\right) + G - \frac{n_{exc}(r,t)}{\tau_{exc}} - F(r)n_{exc}(r,t), \tag{4}$$

where D_{exc} and τ_{exc} are the exciton diffusion coefficient and exciton lifetime at the organic-organic interface, respectively, G is the formation rate of excitons (see also Sec. 2.2), and $F(r)$ is the Förster injection rate of an exciton into the nanocrystal from a distance $r > R$. The Förster injection rate is given by

$$F(r) = F_0\left\{R/\left(r^2 - R^2\right)\right\}^3, \tag{5}$$

where R is the nanocrystal radius, and the Förster constant F_0 is given by $F_0 = 4n_r c\alpha(\omega)\delta^2/3\hbar\omega\varepsilon^2$, which is therefore proportional to the nanocrystal refractive index n_r, the speed of light c, the nanocrystal absorption coefficient $\alpha(\omega)$, the square of the exciton dipole moment, δ, and inversely proportional to the exciton energy $\hbar\omega$ and the square of the dielectric constant of the medium ε [9].

For the hexagonal nanocrystal array in the low nanocrystal concentration limit, we determine analytically the steady-state exciton concentration at the organic-organic interface, and subsequently the exciton injection rate into the nanocrystals, in two extreme cases of the exciton diffusion at the organic-organic interface: in the slow and fast diffusion limits.

In the slow diffusion limit ($D_{exc} \to 0$) the steady-state exciton concentration at a distance r is given by the solution of Eq. (4), namely,

$$n_{exc}^{SD}(r) = G/\left\{(\tau_{exc})^{-1} + F(r)\right\} \tag{6}$$

Therefore, in the slow diffusion limit the exciton injection rate into the nanocrystals is given by

$$C^{SD} = \int_{R+d}^{\infty} F(r)n_{exc}^{SD}(r)2\pi r dr = 2\pi GI, \tag{7}$$

where the integral I is evaluated as

$$I = (R^2/12K^{1/3}) \times \left\{\left(1/\sqrt{3}\right) - 2\sqrt{3}\arctan\left(\left(2X-1\right)/\sqrt{3}\right) + \log\left(\left(1+X\right)^2/\left(1-X+X^2\right)\right)\right\}, \tag{8}$$

with

$$X = K^{1/3}\left\{\left((R+d)/R\right)^2 - 1\right\}, \tag{9}$$

and the constant $K = R^3/(F_0\tau_{exc})$.

In Eq. (7), we use infinity as the upper limit of the integral. This is justified for the hexagonal array of nanocrystals in the low nanocrystal concentration limit, due to the strong power law dependence of r^{-6} of the Förster injection rate in Eq. (5). The lower limit of the integral in Eq. (7) contains the capping layer thickness d, representing the inorganic and/or organic capping layer around the nanocrystals.

In the fast diffusion limit ($D_{exc} \to \infty$) the steady-state exciton concentration n_{exc}^{FD} is assumed to be constant along the organic-organic interface. In order to calculate this exciton concentration, we rewrite Eq. (4) taking into account that the nanocrystals form a hexagonal array at the organic-organic interface. In particular, we integrate over the hexagonal Wigner-Seitz cell around the nanocrystal

and then divide each term by the actual area of the nanocrystal. We find

$$G = (n_{exc}^{FD} / \tau_{exc}) + F n_{exc}^{FD} \rho_1, \quad (10)$$

with constants F and ρ_1 determined by

$$F = \int_{R+d}^{\infty} F(r) 2\pi r dr = \pi F_0 R^3 / \left\{ 2d^2 (2R+d)^2 \right\}, \quad (11)$$

and

$$\rho_1 = \rho / \left\{ 1 - \rho\pi (R+d)^2 \right\}. \quad (12)$$

It follows that in the fast diffusion limit the exciton injection rate into the nanocrystals is given by

$$C^{FD} = F n_{exc} = G / \left\{ \rho + (F\tau_{exc})^{-1} \right\}. \quad (13)$$

Both exciton injection rates into the nanocrystals in the slow (Eq. (7)) and in the fast diffusion (Eq. (13)) limits are overestimated in the large nanocrystal concentration limit at the organic-organic interface. In the low nanocrystal concentration limit, excitons can be only injected into the nearest nanocrystal due to the strong power law distance dependence of the Förster injection rate in Eq. (5). However, in the large nanocrystal concentration limit, when the separation of the nanocrystals appears to be similar to their diameter, the excitons can be injected not only into the nearest nanocrystal, but also into other neighbouring nanocrystals, as illustrated in Fig. 2. At large nanocrystal concentrations, the exciton injection areas of neighbouring nanocrystals overlap. Therefore, in the large nanocrystal concentration limit replacing the upper limit of the integrals in Eqs. (7) and (11) with infinity is no longer justified. We have calculated numerically the injection rates, taking into account the overlap of the nanocrystal injection areas.

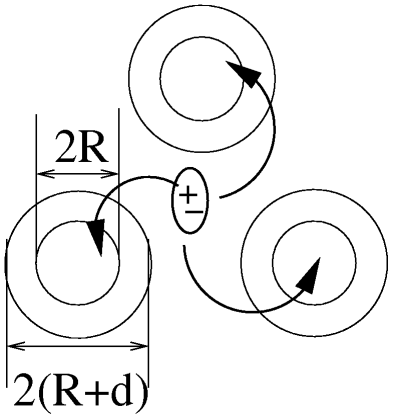

Fig. 2. Illustration of Förster injection of excitons into neighbouring nanocrystals at a large nanocrystal concentration at the organic-organic interface. Top view of a fragment of a hexagonal nanocrystal array with a nanocrystal core radius R and nanocrystal capping layer thickness d .

2.2. Charge transport

In the NC-OLED, the electrons and holes migrate from the metallic electrodes through the organic semiconductor transport layers to the organic-organic interface, where they form bound states (i.e. excitons), as illustrated in Fig. 1. For simplicity we assume that this process can be described by diffusion based charge transport, as the objective of this paper is to give guidance on the arrangement and concentration of the nanocrystals at the organic-organic interface in the NC-OLED. Nevertheless, diffusion based charge transport may be a good approximation in those organic semiconductor systems with large energetic disorder in which transport can be described in terms of hopping between strongly localized states [10]. In these systems, the effects of drift currents become important only when a large electric field exceeding 10^5 V/cm is applied across the whole transport layer. Recent Monte Carlo simulations of charge injection into an organic semiconductor from a metal electrode confirmed that the concentration of injected charge carriers near the electrode is almost three orders of magnitude higher than in the bulk of the organic semiconductor [11]. This suggests that the main drop of the applied potential takes place at the electrode-organic semiconductor interface. Therefore, diffusion based transport may be a good first approximation to describe charge carrier transport through the organic semiconductors in the NC-OLED.

The electron and hole fluxes from the metallic electrodes to the organic interface are described by

$$(D_e / L_e)(n_0 - n_i) = \gamma n_i p_i, \quad (14)$$

$$(D_h / L_h)(p_0 - p_i) = \gamma n_i p_i, \quad (15)$$

where D_e and D_h are the electron and hole diffusion coefficients in the electron and hole organic transport layers, which have thickness L_e and L_h, respectively, n_i and p_i are the electron and hole concentrations at the organic-organic interface, whereas n_0 and p_0 are the electron and hole concentrations at the cathode and anode, respectively. In the steady-state, the charge flux to the interface is compensated by the rate of exciton formation $G = \gamma n_i p_i$, as described by Eqs. (14) and (15). We assume that the charge carriers and the excitons do not interact and that the densities of electrons and holes are constant along the organic-organic interface. The latter assumption is justified because the organic semiconductor layers are at least an order of magnitude thicker than the diameter of the nanocrystals. In addition, we assume that the transport energy levels of the organic electron and hole transport layers are such that they are also blocking layers for the other type of charge carriers. Therefore, it is possible to neglect the presence of minority carriers in the system. Subsequently, excitons can only form at the organic-organic interface.

In the NC-OLED, the exciton formation rate at the organic-organic interface is determined by the solution of Eqs. (14) and (15). It is given by

$$\begin{aligned} G &= \gamma n_i p_i \\ &= 0.5\gamma\left\{Pp_0^2 + Nn_0^2 - PNp_0n_0 \right. \\ &\left. -\sqrt{\left(Pp_0^2 + Nn_0^2 + PNp_0n_0\right)^2 - 4PNp_0^2n_0^2}\right\}, \end{aligned} \tag{16}$$

where the dimensionless parameters N and P are defined by $N = D_e/(\gamma L_e n_0)$ and $P = D_h/(\gamma L_h p_0)$. The exciton formation rate constant γ contains a geometrical factor proportional to the nanocrystal concentration at the organic-organic interface, as the exciton formation is restricted to the interface area which is not covered by nanocrystals:

$$\gamma = \gamma_0\left\{1 - \rho\pi(R+d)^2\right\}, \tag{17}$$

where γ_0 is the exciton formation rate constant.

2.3. Light intensity and quantum efficiency

We analyse the performance of the NC-OLED by studying its light emission intensity and quantum efficiency. The light emission intensity is proportional to the number of photons emitted per unit time, e.g. the steady-state solution of Eqs. (1)-(3), and it should be multiplied by the photon energy $\hbar\omega_{ph}$:

$$I = (N_1/\tau)\hbar\omega_{ph} = \rho\{C/(1+C\tau)\}\hbar\omega_{ph}. \tag{18}$$

The NC-OLED quantum efficiency is given by the number of emitted photons divided by the number of injected electrons (electron flux), and it is determined as

$$\eta = (N_1/\tau)/\{(D_e/L_e)(n_0 - n_i)\}. \tag{19}$$

2.4. Parameter set

We determine the parameter set for our model NC-OLED by choosing candidate materials of CdSe nanocrystals and MEH-PPV polymers for the organic semiconductors.

The radiative recombination time for excitons in CdSe nanocrystals is of the order of 10 ns [12], with a typical nanocrystal radius of the order of $R = 1\,\text{nm}$. The emitted photon energy strongly varies with nanocrystal radius, but for OLEDs in display technology this energy value is typically between 2.0 and 2.7 eV. For simplicity, we use the value of $\hbar\omega_{ph} = 2.5\,\text{eV}$ in this paper when calculating the light emission intensity of the NC-OLED. We use the value of $d = 1\,\text{nm}$ for the capping layer thickness around the nanocrystals.

In the vicinity of the nanocrystal, the exciton Förster energy transfer is equal to $F(r = R+d) = F_0/27R^3$ if $R = d$ (see parameter choice in this section), which on the other hand is approximately equal to 0.1ps^{-1} [9]. Therefore the Förster injection constant F_0 can be estimated to be around $1\text{nm}^3/\text{ps}$.

The exciton lifetime τ_{exc} in MEH-PPV is of the order of 100 ps [13] and we use this value for the exciton lifetime along the organic-organic interface. It has been shown that MEH-PPV can be synthesized either as a hole or electron transport layer [14]. However, for simplicity, we only consider in this paper the symmetric case for the kinetic coefficients for electrons and holes, e.g. when they are equal in both types of organic semiconductor ($D = D_e = D_h$, $L = L_e = L_h$, and $n_0 = p_0$). Typical values for the diffusion constant, film thickness and charge concentration at the electrode are $D \approx 10^{-6}\,\text{cm}^2/\text{s}$ (using the Einstein relation $D = \mu k_B T/e$ at room temperature with a mobility of charge carriers in the organic film of $\mu = 10^{-5}\,\text{cm}^2/\text{Vs}$ [15]), $L = 50\,\text{nm}$ [1], and $n_0 = 10^{18}\,\text{cm}^{-3}$, respectively.

The exciton formation rate constant γ_0 can be estimated with the help of the Langevin recombination rate given by $\hat{\gamma} = e\mu/\varepsilon\varepsilon_0$ [14]. An order of magnitude estimate for $\hat{\gamma}$ is $10^{-2}\,\text{nm}^3/\text{ps}$ using the mobility of $\mu = 10^{-5}\,\text{cm}^2/\text{Vs}$ and the dielectric constant $\varepsilon = 3$. Then the exciton formation rate γ_0 is calculated by multiplying $\hat{\gamma}$ with the typical distance between electrons and holes when they form excitons at the interface. The latter quantity is estimated to be of the order of $d_{exc} \approx 1\,\text{nm}$ using the binding energy for excitons of $E_b = 0.4\,\text{eV}$ [16]. Therefore, the exciton formation rate constant γ_0 can be estimated to be of the order of $10^{-2}\,\text{nm}^4/\text{ps}$.

3. Results and discussion

The NC-OLED light emission intensity can be tuned by changing the nanocrystal concentration at the organic-organic interface, as illustrated in Fig. 3. At low nanocrystal concentrations, when the nanocrystal separation is large, the light emission intensity is small. This is due to the slight possibility that excitons are Förster injected into the nanocrystals in this case. The Förster injection rate has a strong power law dependence on distance - r^{-6} (Eq. (5)), and therefore even in the fast exciton diffusion limit the light emission intensity approaches zero when the separation of nanocrystals becomes larger than 15 nm in the NC-OLED (Fig. 3). There is a monotonic increase in light emission intensity when the separation between the nanocrystals at the

organic-organic interface is decreased, as seen in Fig. 3. This increase in intensity saturates, and then drops at large nanocrystal concentrations (>0.05 nm^{-2}), when the nanocrystals are very close to each other at the organic-organic interface. This drop in brightness is due to the interplay between the increasing efficiency of exciton injections into nanocrystals and the decreasing number of excitons generated at the organic-organic interface with increasing nanocrystal concentration. The decreasing number of excitons with increasing nanocrystal concentration is due to the fact that exciton formation is confined to the area which is not covered by nanocrystals at the organic-organic interface.

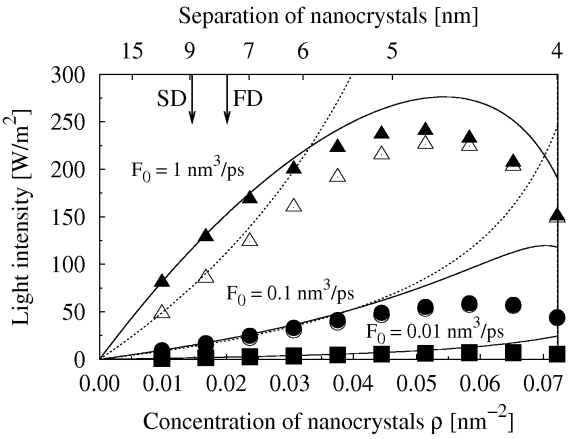

Fig. 3. Light emission intensity of a NC-OLED as a function of the nanocrystal concentration at the organic-organic interface. Open and solid triangles, circles, and squares represent numerical data for Förster prefactor F_0 = 1, 0.1, and 0.01 nm^3/ps in slow and fast diffusion limits, respectively. Other parameters were chosen as discussed in Sec. 2.4. Dashed and solid lines represent analytical solutions calculated by the injection rates in Eqs. (7) and (13) in the fast and slow diffusion limits, respectively. Vertical arrows illustrate limits, where analytical solutions are expected to deviate from numerical solutions due to overlap of neighbouring nanocrystal exciton injection areas.

The quantum efficiency of the NC-OLED is a monotonically increasing function of the nanocrystal concentration at the organic-organic interface, as seen in Fig. 4. At low nanocrystal concentrations, when the separation between the nanocrystals is large, only a small amount of excitons are injected into the nanocrystals, due to the strong power law dependence of the Förster injection rate on distance. Increasing the nanocrystal concentration contributes to a better injection efficiency of excitons into the nanocrystals. Therefore, the NC-OLED quantum efficiency is a monotonically increasing function of the nanocrystal concentration at the organic-organic interface.

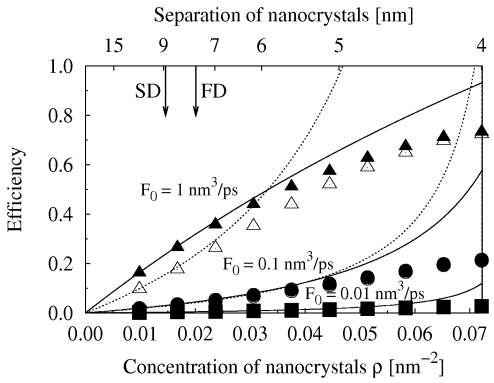

Fig. 4. Quantum efficiency of a NC-OLED as a function of the nanocrystal concentration at the organic-organic interface. Open and solid triangles, circles, and squares represent numerical data for the Förster prefactor F_0 = 1, 0.1, and 0.01 nm^3/ps in the slow and fast diffusion limits, respectively. Other parameters were chosen as discussed in Sec. 2.4. Dashed and solid lines represent analytical solutions calculated by the injection rates in Eqs. (7) and (13) in the fast and slow diffusion limits, respectively. Vertical arrows illustrate limits, where analytical solutions expect to deviate from numerical solutions due to overlap of neighbouring nanocrystal exciton injection areas.

Our results demonstrate that the NC-OLED light emission intensity and quantum efficiency are mostly affected by the efficiency of the Förster injection of excitons into nanocrystals, as seen for varying values of the Förster constant F_0 in Figs. 3 and 4. An order of magnitude increase in this constant contributes to a significant increase both in the light emission intensity and quantum efficiency. Other parameters affecting the efficiency of the Förster injection are the nanocrystal capping layer thickness d and the exciton lifetime τ_{exc} at the organic-organic interface. In order to increase the NC-OLED light emission intensity and quantum efficiency, one should aim for thinner nanocrystal shell thicknesses, and one should employ those organic interfaces where the exciton recombination rate is considerably larger than the exciton injection rate into the nanocrystals [17].

The similarity between the NC-OLED light emission intensity in the slow and fast exciton diffusion limits in Fig. 3 indicates that the NC-OLED performance is not significantly sensitive to the exciton kinetics at the organic-organic interface. We also note that the analytical approach in the fast diffusion limit describes reasonably well the NC-OLED light emission intensity and quantum efficiency even at large nanocrystal concentrations, as can be observed in Figs. 3 and 4.

The NC-OLED performance is also affected by the kinetic coefficients determining the charge transport in the organic semiconductors, such as the charge carrier diffusion constant, the charge carrier concentration at the metal electrodes and the organic film thickness. Our results provide guidance on the general trends to be followed for the material choice of the NC-OLED.

Namely, it is preferable to have an organic semiconductor in which the carrier diffusion constant is large and also the thickness of this material should be as slim as possible [17].

4. Conclusions

We have developed a rate equation model to study the light emission intensity and quantum efficiency of a hybrid organic light-emitting diode, when the nanocrystals are embedded between the hole and electron transport layers of organic semiconductors (NC-OLED). In our model, the Förster injection of excitons from the organic-organic interface is determined by the exciton formation and the exciton kinetics at the organic-organic interface, which is controlled by the diffusion based transport of charge carriers through the organic semiconductors from the metallic electrodes to the organic-organic interface. We have found that the NC-OLED light emission intensity can be optimized by choosing the right nanocrystal concentration at the organic-organic interface. The NC-OLED performance is mainly affected by the efficient Förster injection of excitons from the organic semiconductors into the nanocrystals, and it is less sensitive to the exciton kinetics at the organic-organic interface.

Acknowledgements

This research is funded by Hewlett-Packard Laboratories (Palo Alto, California). Valuable discussions with Jim Brug, C.C. Yang, Gary Gibson, and Chris Nauka are gratefully acknowledged. The calculations were performed at the Materials Modelling Laboratory (University of Oxford).

References

[1] S. Coe, W-K. Woo, M. Bawendi, V. Bulovic, Nature **420**, 800 (2002).
[2] N. Tessler, V. Medvedev, M. Kazes, S. Kan, U. Banin, Science **295,** 1506 (2002).
[3] J. Zhao, J. Zhang, C. Jiang, J. Bohnenberger, T. Basche, A. Mews, J. Appl. Phys. **96**, 3206 (2004).
[4] T. Tsutsui, Nature **420**, 752 (2002).
[5] A. Javier, C.S. Yun, J. Sorena, G.F. Strouse, J. Phys. Chem. B **107**, 435 (2003).
[6] H. Baessler, Phys. Stat. Sol. (b) **175**, 15 (1993).
[7] Al. Efros, M. Rosen, Phys. Rev. Lett. **78**, 1110 (1997).
[8] M. Drndic, M. V. Jarosz, N. Y. Morgan, M. A. Kastner, M. G. Bawendi, J. Appl. Phys. **92**, 7498 (2002) 7498.
[9] A. Shik, G. Konstantatos, E. H. Sargent, H. E. Ruda, J. Appl. Phys. **94** , 4066 (2003).
[10] K. Kohary, H. Cordes, S.D. Baranovski, P. Thomas, S. Yamasaki, F. Hensel, J.-H. Wendorff, Phys. Rev. B **63**, 094202 (2001).
[11] E. Tsymbal (private communication).
[12] S. A. Crooker, T. Barrick, J. A. Hollingsworth, V. I. Klimov, Appl. Phys. Lett. **82**, 2793 (2003).
[13] G. D. Hale, S. J. Oldenburg, N. J. Halas, Appl. Phys. Lett. **71**, 1483 (1997).
[14] J. C. Scott, P. J Brock, J. R. Salem, S. Ramos, G. G. Malliaras, S.A. Carter, L. Bozano, Synth. Met. **111-112**, 289 (2000).
[15] A. R. Inigo, C. C. Chang, W. Fann, J. D. White, Y. S. Huang, U.S. Jeng, H. S. Sheu, K. Y. Pent, S. A. Chen, Adv. Mater. **17**, 1835 (2005).
[16] S. F. Alvarado, P. F. Seidler, D. G. Lidzey, D. C. Bradley, Phys. Rev. Lett. **81**, 1082 (1998).
[17] K. Kohary, V.M. Burlakov, D.G. Pettifor, J. Appl. Phys. (accepted).

*Corresponding author: krisztian.kohary@materials.ox.ac.uk